RSC Advances

PAPER

View Article Online
View Journal | View Issue

Open Access Article. Published on 18 January 2017. Downloaded on 2/19/2025 8:11:18 PM.
This article is licensed under a Creative Commons Attribution 3.0 Unported Licence.

Cite this: *RSC Adv.*, 2017, **7**, 6089

Bis[1]benzothieno[2,3-*d*:2′,3′-*d*′]anthra[1,2-*b*:5,6-*b*′]dithiophene: synthesis, characterization, and application to organic field-effect transistors†

Keita Hyodo,[a] Hideki Hagiwara,[b] Ryota Toyama,[a] Hiroki Mori,[c] Shin-ichi Soga[d] and Yasushi Nishihara*[c]

Received 28th November 2016
Accepted 7th January 2017

DOI: 10.1039/c6ra27455b

www.rsc.org/advances

We report the straightforward synthetic method and characterization of bis[1]benzothieno[2,3-*d*:2′,3′-*d*′]anthra[1,2-*b*:5,6-*b*′]dithiophene (BBTADT) having nine aromatic rings fused without solubilizing groups. The highest mobility of fabricated OFETs utilizing BBTADT exhibited 2.7 × 10^{-2} cm^2 V^{-1} s^{-1} in polycrystalline films formed by vapor deposition, depending on the annealing temperatures of a substrate.

Organic field-effect transistors (OFETs) have attracted much attention as next-generation electronic devices because of their advantageous features which involve flexibility, light weight, low cost, ease of design, printability, and so on.[1] To ensure the practical application of electronic paper, sensors, and radio frequency identification (RFID) tags, important factors are not only high carrier mobility and low voltage operation but air stability and thermal durability in thin films of OFETs.[2] In the field of the small molecular materials, the highest hole mobility is over 40 cm^2 V^{-1} s^{-1} in single-crystal OFETs based on 2,7-dioctyl[1]benzothieno[3,2-*b*][1]benzothiophene (C8-BTBT).[3] Despite high hole mobility, C8-BTBT exhibited low thermal stability and long-term durability, presumably owing to the small number of the fused aromatic rings.[4]

Recently, Takeya and co-workers reported N-shaped 3,11-didecyldinaphtho[2,3-*d*:2′,3′-*d*′]benzo[1,2-*b*:4,5-*b*′]dithiophene (C10-DNBDT-NW) with seven fused aromatic rings exhibiting high hole mobility of 16 cm^2 V^{-1} s^{-1} in single-crystal OFETs formed by edge-cast method.[5] Moreover, Takimiya and co-workers developed 2,10-diphenylbis[1]benzothieno[2,3-*d*:2′,3′-*d*′]naphtho[2,3-*b*:6,7-*b*′]dithiophene (DPh-BBTNDT) with eight fused aromatic rings, which also showed high hole mobility of 7 cm^2 V^{-1} s^{-1} in polycrystalline films fabricated by vapor deposition.[6] Importantly, OFET devices based on each material have achieved high thermal stability under 200 °C, low-voltage operation, and long-term durability because highly fused aromatic compounds have a rigid structure and thus enhance the intermolecular interactions between the neighbouring molecules.

Although small molecules with extended π-electron systems are promising materials for high-performance OFET devices, it is quite difficult to synthesize due to low solubility of the precursors and the products. In fact, there are a few reports of the materials with fused aromatic rings over nine. For instance, Kubozono and co-workers systematically investigated [*n*]phenacenes (*n* = 5 to 9) composed of benzene rings with W-shaped structures, which were readily synthesized through photocyclization.[7] The mobility become higher along with an extension of π-electron systems, especially, the single crystal of [9]phenacene-based OFET devices showed very high mobility up to 18 cm^2 V^{-1} s^{-1} with ZrO_2 gate dielectrics. Another report of the nine aromatic rings-fused thienoacenes is 7,15-dialkyl- or dialkoxy-bis[1]benzothieno[2,3-*d*:2′,3′-*d*′]thieno[2,3-*b*:2′,3′-*b*′]benzo[1,2-*b*:4,5-*b*′]dithiophene.[8] An alkyl or alkoxy group improves the solubility. The fabricated OFET devices based on undecyl-substituted thienoacene exhibited high mobility over 1 cm^2 V^{-1} s^{-1}. Unfortunately, they failed to synthesize unsubstituted nine ring-fused thienoacene due to the lower nucleophilicity. Therefore, it is worth developing the novel molecules with extended π-electron systems as many as nine fused aromatic rings from viewpoints of materials science and synthetic chemistry.

Previously, we have developed an efficient synthetic method of phenanthro[1,2-*b*:8,7-*b*′]dithiophene (PDT) as phenacene-type molecule through sequential three reactions: palladium-catalyzed cross-coupling reactions of 3-formylthienylboron or -zinc reagents and 1,4-dibromobenzene, epoxidation of aldehyde moieties, and Lewis-acid catalyzed Friedel–Crafts type intramolecular cycloaromatization reaction.[9] Moreover, the fabricated OFET devices based on didodecyl-substituted PDT (C12-PDT) exhibited high hole mobility of 1.75 cm^2 V^{-1} s^{-1} in

[a]*Division of Earth, Life, and Molecular Sciences, Graduate School of Natural Science and Technology, Okayama University, 3-1-1 Tsushimanaka, Kita-ku, Okayama 700-8530, Japan. E-mail: ynishiha@okayama-u.ac.jp*

[b]*Tosoh Organic Chemical, 4988 Kaisei-cho, Shunan, Yamaguchi 746-0006, Japan*

[c]*Research Institute for Interdisciplinary Science, Okayama University, 3-1-1 Tsushimanaka, Kita-ku, Okayama 700-8530, Japan*

[d]*Tosoh, 4560 Kaisei-cho, Shunan, Yamaguchi 746-8501, Japan*

† Electronic supplementary information (ESI) available. See DOI: 10.1039/c6ra27455b

Open Access Article. Published on 18 January 2017. Downloaded on 2/19/2025 8:11:18 PM.
This article is licensed under a Creative Commons Attribution 3.0 Unported Licence.

polycrystalline films on Si/SiO_2 substrate.[10] However, absolute threshold voltage was very high value of 68 V due to the high energy barrier between the work function of gold (*ca.* 5.1 eV)[11] as source and drain electrodes and ionization potential of C12-PDT (5.8 eV). We have achieved higher mobility of 2.19 $cm^2 V^{-1} s^{-1}$ and lower absolute threshold voltage of 12 V when HfO_2 was employed as the gate dielectrics. Herein, we report the novel unsubstituted nine aromatic rings-fused thienoacene molecule, bis[1]benzothieno[2,3-*d*:2′,3′-*d*′]anthra[1,2-*b*:5,6-*b*′]dithiophene (BBTADT) incorporating an anthracene moiety in a molecular centre in order to increase the HOMO energy level, which can enhance the hole injection from the gold electrodes.

The development of an efficient synthetic route to BBTADT without the formation of structural isomers is required because separation of isomers seems to be quite difficult due to their low solubility. Therefore, based on our retrosynthetic analysis (Scheme 1), an anthracene moiety is formed by Lewis acid-catalyzed cycloaromatization reaction of epoxide as the precursor because a rigid anthracene-containing intermediates would show low solubility. An epoxide moiety is readily synthesized from aldehyde using trimethylsulfonium iodide in the presence of a base. Compound **3** is formed by palladium-catalyzed Negishi coupling reaction of the *in situ* generated zinc reagent from **1** with 2,5-diiodo-1,4-benzenedicarboxaldehyde (**2**). Dialdehyde **2** is the key starting material in order to prevent the formation of cyclized structural isomers. According to synthetic protocol in the literatures,[12,13] compounds **1** and **2** were prepared in 47% and 46%, respectively (Schemes S1 and S2†). A synthetic route of BBTADT is summarized in Scheme 2. Palladium-catalyzed Negishi coupling reaction of **2** with 2 equiv. of zinc reagent, derived from deprotonation[14] and the subsequent zincation of **1** afforded the coupled product **3** in 74% yield. An sequential epoxidation of **3** furnished the desired product **4** in 88% yield. Finally, BBTADT was obtained in 33% yield through indium-catalyzed Friedel–Crafts type intramolecular cyclo-aromatization reaction and purification by vacuum sublimation twice. BBTADT showed a quite low solubility in common organic solvents such as toluene, chloroform, chlorobenzene, and so on. Therefore, the formation of BBTADT was identified by elemental analysis. Furthermore, we carried out the measurements of thermogravimetric analysis (TGA) and differential scanning calorimetry (DSC) in order to evaluate the thermal stability of BBTADT (Fig. S3†). To our delight, the temperature of 5% weight loss was 464 °C and no transition

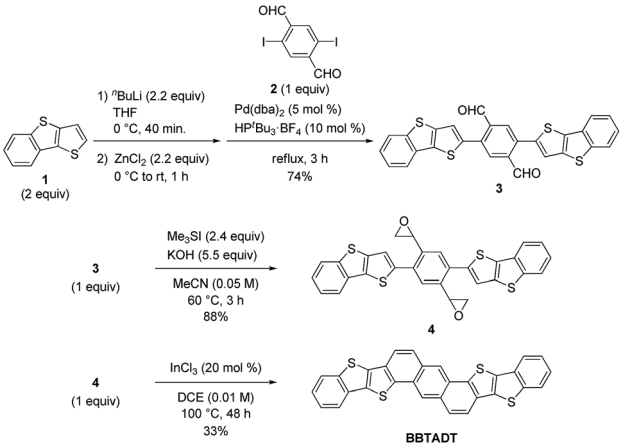

Scheme 2 Synthetic procedure of BBTADT.

peaks up to 300 °C was observed, indicating that BBTADT has high thermal stability due to its highly π-electron systems.

In order to evaluate physicochemical properties of BBTADT, the thin film of BBTADT was prepared by vapor deposition at the rate of 0.1 Å s^{-1} on a quartz glass substrate and the UV-vis absorption spectrum of its thin film was measured. Obtained absorption spectrum is shown in Fig. 1. The spectrum shape is similar to that of anthra[1,2-*b*:5,6-*b*′]dithiophene (ADT) consisting of five aromatic rings. Therefore, electronic structure of BBTADT was strongly depend on the ADT framework.[15] The maximum absorption wavelength of BBTADT was observed at 431 nm, and the energy bandgap estimated from absorption edge (501 nm) was 2.5 eV, which is suitable to show air stability in OFET devices.

The OFET devices based on BBTADT were fabricated by vapor deposition with a top-contact/bottom-gate configuration on octyltrichlorosilane (OTS)-treated Si/SiO_2 substrate. The fabricated thin films were thermally annealed at 100, 150, and 200 °C in glove box for 30 min. The gold source and drain electrodes were deposited through a shadow mask by vacuum deposition, which gave a channel length (L) of 100 μm and a width (W) of 2 mm. The measurements were carried out under ambient conditions in the dark. The representative transfer and output curves were shown in Fig. 2 and the obtained OFET properties were summarized in the Table 1. The OFET devices based on as-deposited thin films exhibited the highest hole mobility of 2.7 × 10^{-2} $cm^2 V^{-1} s^{-1}$, low threshold voltage of −9 V, and high on/off current ratio up to 10^7. After the thermal

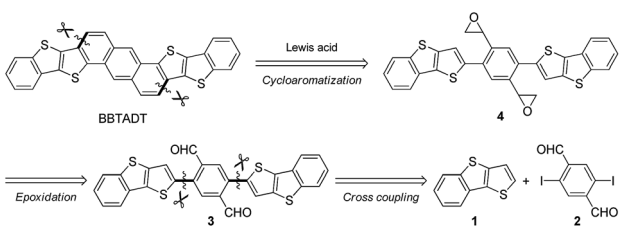

Scheme 1 Retrosynthetic analysis of BBTADT.

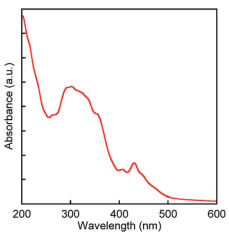

Fig. 1 UV-vis absorption spectrum of thin films based on BBTADT.

This journal is © The Royal Society of Chemistry 2017

Open Access Article. Published on 18 January 2017. Downloaded on 2/19/2025 8:11:18 PM.
This article is licensed under a Creative Commons Attribution 3.0 Unported Licence.

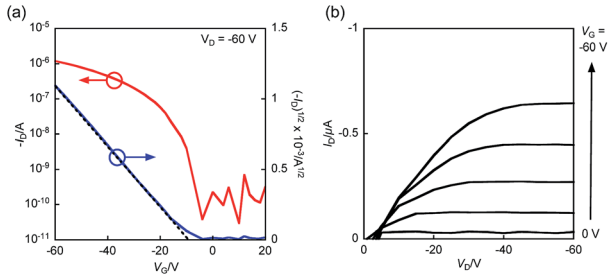

Fig. 2 (a) Transfer and (b) output curves of BBTADT-based OFET devices in as-deposited thin films.

annealing at 100 °C, FET characteristics slightly decreased to 1.3×10^{-2} cm^2 V^{-1} s^{-1}. Further increasing the annealing temperature at 150 °C and 200 °C, no FET responses were observed, indicating that the change of the molecular orientation from edge-on to face-on in thin films as increasing the temperature of thermal annealing (*vide infra*).

In general, thermal annealing process can rearrange the order of molecules in thin films, which may enhance the FET performance. In order to investigate the surface morphology and the molecular orientation in thin films, atomic force microscopy (AFM) and X-ray diffraction (XRD) were measured, shown in Fig. 3 and 4, respectively. 2 μm × 2 μm topographic AFM images showed granulose grains as observed for many related polycrystalline organic semiconductors. In as-deposited films, a lot of small grains and clear grain boundaries were observed, which often suppress an effective carrier transport. The grain size was not significantly enlarged after thermal annealing at 100 °C. Increasing the annealing temperature at 150 and 200 °C, the grain size became bigger, which might enhance the effective carrier transport. However, this hypothesis is not consistent with the observed FET properties.

In terms to the out-of-plane XRD pattern, as-deposited films showed weak and only second order of (00*l*) diffraction peaks, suggesting the low crystallinity of thin films. The lattice *d*-spacing estimated from (001) diffraction peaks at $2\theta = 4.8°$ was 18.3 Å, which is shorter than the molecular length of BBTADT calculated from theoretically optimized molecular geometry (Fig. S4†). Therefore, BBTADT showed an edge-on orientation in thin films and a tilt angle against the substrate is 31° (Fig. S4†). On the other hand, *d*-spacing of 3.4 Å was estimated from the diffraction peaks at $2\theta = 25.9°$, which might be derived from π–π stacking structure with a face-on arrangement. The low crystallinity and the mixture of edge-on and face-on orientations lead to a relatively low mobility of BBTADT-based OFET

Table 1 FET properties of BBTADT-based OFET devices on OTS-modified Si/SiO_2 substrates

Compound	T_{anneal} (°C)	μ (cm^2 V^{-1} s^{-1})	V_{th} (V)	$I_{on/off}$
BBTADT	As depo.	2.7×10^{-2}	−9	10^3 to 10^7
	100	1.3×10^{-2}	−8	10^3 to 10^5
	150	No FET characteristics		
	200	No FET characteristics		

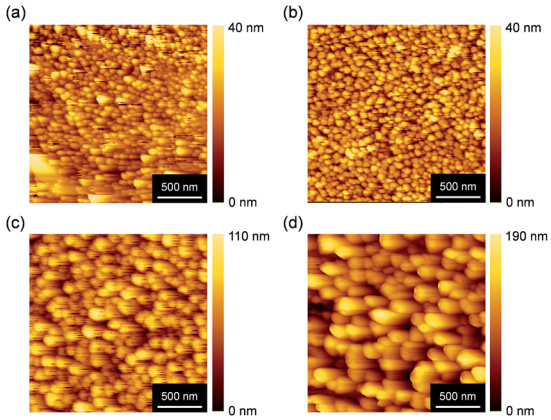

Fig. 3 Topographic AFM images of BBTADT thin film on OTS-modified Si/SiO_2 substrate after thermal annealing at (a) as-deposited, (b) 100 °C, (c) 150 °C, and (d) 200 °C.

devices as-deposited films. Surprisingly, the large temperature dependence of molecular orders was observed, in spite of very high thermal stability of BBTADT. As increasing the annealing temperature, the intensity of the diffraction peaks derived from a face-on orientation was increased, and (00*l*) diffraction peaks disappeared after thermal annealing at 200 °C. Such complete face-on orientation is unfavorable for OFET, leading to poor carrier transport. Furthermore, no peaks were observed at the in-plane direction with or without thermal annealing, indicating that no ordered structure along the in-plane direction is present in the solid state, originating from its intrinsically low crystallinity. Thus, the thermal annealing process could not enhance the FET performance in this study, and as-deposited film exhibited the highest hole mobility. From these results, we concluded that the face-on orientation in BBTADT film is a thermally stable state, although the reason is still unclear.

In conclusion, we have developed a novel synthetic method of BBTADT as nine aromatic rings-fused thienoacene without the formation of structural isomers. The fabricated OFET devices based on BBTADT exhibited typical p-channel and normally-off behaviors under ambient conditions in the dark. The maximum hole mobility was 2.7×10^{-2} cm^2 V^{-1} s^{-1} in as-deposited thin films. Moreover, low-voltage operation and high current on/off ratio have been achieved. After thermal annealing over 150 °C, no FET response was observed because the

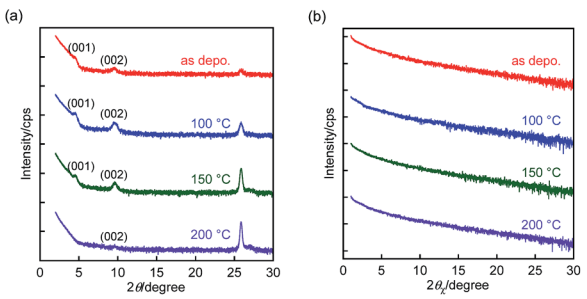

Fig. 4 (a) Out-of-plane and (b) in-plane XRD patterns of BBTADT thin films on OTS-modified Si/SiO_2 substrate.

Open Access Article. Published on 18 January 2017. Downloaded on 2/19/2025 8:11:18 PM.
This article is licensed under a Creative Commons Attribution 3.0 Unported Licence.

molecular orientation showed mainly face-on, which is not effective to the carrier transport. Such behavior is unusual in related organic semiconductors with the extended π-electron system. Thus, this study may provide new design concept toward high-performance OFET materials based on polycyclic aromatic compounds. In order to develop the high-performance materials for FET, the introduction of alkyl substituents at the molecular long-axis direction is one of the effective strategy to enhance the crystallinity and molecular ordering, because long alkyl substituents lead to a fastener effect, which can fasten the π-core of the molecule through van der Waals interaction between alkyl chains.[5,10,16] Moreover, diphenyl-substituted compounds along the molecular long-axis direction typically have higher thermal stability in themselves and thin film compared with the corresponding parent molecules.[6,17] Therefore, the synthesis of dialkyl and diphenyl-substituted BBTADT are currently underway in our laboratory.

Acknowledgements

This work was partly supported by ACT-C, JST and a Grant-in-Aid for Scientific Research (KAKENHI) (No. 15J07968) from JSPS, and the Program for Promoting the Enhancement of Research Universities from MEXT and a Special Project of Okayama University. The authors gratefully thank Prof. Naoshi Ikeda (Okayama University) for the measurements of AFM images, Prof. Tetsuya Uchida (Okayama University) for the measurements of TGA, Prof. Tsutomu Ono and Prof. Takaichi Watanabe for the measurements of DSC, and Ms M. Kosaka and Mr M. Kobayashi at the Department of Instrumental Analysis, Advanced Science Research Center, Okayama University, for the measurement of elemental analyses, respectively. The SC-NMR Laboratory of Okayama University for the NMR spectral measurements is gratefully acknowledged.

References

1 M. L. Hammock, A. Chortos, B. C.-K. Tee, J. B.-H. Tok and Z. Bao, *Adv. Mater.*, 2013, **25**, 5997.
2 H. Dong, X. Fu, J. Liu, Z. Wang and W. Hu, *Adv. Mater.*, 2013, **25**, 6158.
3 Y. Yuan, G. Giri, A. L. Ayzner, A. P. Zoombelt, S. C. B. Mannsfeld, J. Chen, D. Nordlund, M. F. Toney, J. Huang and Z. Bao, *Nat. Commun.*, 2014, **5**, 3005.
4 H. Ebata, T. Izawa, E. Miyazaki, K. Takimiya, M. Ikeda, H. Kuwabara and T. Yui, *J. Am. Chem. Soc.*, 2007, **129**, 15732.
5 C. Mitsui, T. Okamoto, M. Yamagishi, J. Tsurumi, K. Yoshimoto, K. Nakahara, J. Soeda, Y. Hirose, H. Sato, A. Yamano, T. Uemura and J. Takeya, *Adv. Mater.*, 2014, **26**, 4546.
6 M. Abe, T. Mori, I. Osaka, K. Sugimoto and K. Takimiya, *Chem. Mater.*, 2015, **27**, 5049.
7 (*a*) Y. Kubozono, X. He, S. Hamao, K. Teranishi, H. Goto, R. Eguchi, T. Kambe, S. Gohda and Y. Nishihara, *Eur. J. Inorg. Chem.*, 2014, 3806; (*b*) Y. Shimo, T. Mikami, H. T. Murakami, S. Hamao, H. Goto, H. Okamoto, S. Gohda, K. Sato, A. Cassinese, Y. Hayashi and Y. Kubozono, *J. Mater. Chem. C*, 2015, **3**, 7370; (*c*) Y. Shimo, T. Mikami, S. Hamao, H. Goto, H. Okamoto, R. Eguchi, S. Gohda, Y. Hayashi and Y. Kubozono, *Sci. Rep.*, 2016, **6**, 21008.
8 Y. Xiong, X. Qiao, H. Wu, Q. Huang, Q. Wu, J. Li, X. Gao and H. Li, *J. Org. Chem.*, 2014, **79**, 1138.
9 K. Hyodo, H. Nonobe, S. Nishinaga and Y. Nishihara, *Tetrahedron Lett.*, 2014, **55**, 4002.
10 Y. Kubozono, K. Hyodo, H. Mori, S. Hamao, H. Goto and Y. Nishihara, *J. Mater. Chem. C*, 2015, **3**, 2413.
11 H. B. J. Michaelson, *J. Appl. Phys.*, 1977, **48**, 4729.
12 For the synthesis of **1**. (*a*) H. Tian, Y. Han, C. Bao, D. Yan, Y. Geng and F. Wang, *Chem. Commun.*, 2012, **48**, 3557; (*b*) P. Y. Huang, L. H. Chen, Y. Y. Chen, W. J. Chang, J. J. Wang, K. H. Lii, J. Y. Yan, J. C. Ho, C. C. Lee, C. Kim and M. C. Chen, *Chem.–Eur. J.*, 2013, **19**, 3721.
13 For the synthesis of **2**. (*a*) G. Gaefke, V. Enkelmann and S. Höger, *Synthesis*, 2006, **17**, 2971; (*b*) S. Seo and T. J. Marks, *Chem.–Eur. J.*, 2010, **16**, 5148.
14 P.-Y. Huang, L.-H. Chen, Y.-Y. Chen, W.-J. Chang, J.-J. Wang, K.-H. Lii, J.-Y. Yan, J.-C. Ho, C.-C. Lee, C. Kim and M.-C. Chen, *Chem.–Eur. J.*, 2013, **19**, 3721.
15 (*a*) A. Pietrangelo, M. J. Maclachlan, M. O. Wolf and B. O. Patrick, *Org. Lett.*, 2007, **9**, 3571; (*b*) A. Pietrangelo, B. O. Patrick, M. J. MacLachlan and M. O. Wolf, *J. Org. Chem.*, 2009, **74**, 4918.
16 M.-J. Kang, I. Doi, H. Mori, E. Miyazaki, K. Takimiya, M. Ikeda and H. Kuwabara, *Adv. Mater.*, 2011, **23**, 1222.
17 M.-J. Kang, E. Miyazaki, I. Osaka, K. Takimiya and A. Nakao, *ACS Appl. Mater. Interfaces*, 2013, **5**, 2331.

 This journal is © The Royal Society of Chemistry 2017